

EXPLORING THE CASIMIR FORCE AT ONE-LOOP LEVEL

A THESIS SUBMITTED TO
THE GRADUATE SCHOOL OF NATURAL AND APPLIED SCIENCES
OF
MIDDLE EAST TECHNICAL UNIVERSITY

BY

NERGIS NEVRA YALÇIN

IN PARTIAL FULFILLMENT OF THE REQUIREMENTS
FOR
THE DEGREE OF MASTER OF SCIENCE
IN
PHYSICS

FEBRUARY 2021

Approval of the thesis:

EXPLORING THE CASIMIR FORCE AT ONE-LOOP LEVEL

submitted by **NERGIS NEVRA YALÇIN** in partial fulfillment of the requirements for the degree of **Master of Science in Physics Department, Middle East Technical University** by,

Prof. Dr. Halil Kalıpçılar
Dean, Graduate School of **Natural and Applied Sciences**

Prof. Dr. Altuğ Özpineci
Head of Department, **Physics**

Prof. Dr. İsmail Turan
Supervisor, **Physics, METU**

Examining Committee Members:

Assoc. Prof. Dr. Levent Selbuz
Physics Engineering, Ankara University

Prof. Dr. İsmail Turan
Physics, METU

Prof. Dr. Tahmasib Aliyev
Physics, METU

Date: 12.02.2021

I hereby declare that all information in this document has been obtained and presented in accordance with academic rules and ethical conduct. I also declare that, as required by these rules and conduct, I have fully cited and referenced all material and results that are not original to this work.

Name, Surname: Nergis Nevra Yalçın

Signature :

ABSTRACT

EXPLORING THE CASIMIR FORCE AT ONE-LOOP LEVEL

Yalçın, Nergis Nevra

M.S., Department of Physics

Supervisor: Prof. Dr. İsmail Turan

February 2021, 44 pages

Casimir force was first discovered by Hendrik Casimir in 1948 and it is a physical effect originally proposed for the two neutral conducting parallel plate geometry whose successful measurement by Lamoreaux *et al.* took almost five decades. Basically, it describes the existence of a force due to the quantum vacuum itself. For years, studies have been concentrated on the compatibility of the theory, namely the quantum electrodynamics, with experimental outcomes. Over the years the subject has grown tremendously and even became a topic of interdisciplinary studies within physics as well as engineering. After Lamoreaux's measurement with experimental errors taken under control, many studies have been inspired by this and later extended to involve different geometries including spherical and cylindrical surfaces which are proven to be more efficient. The main objective of the thesis is two-fold. Firstly, we aim to understand the origin of the casimir force at the most fundamental level through the use of quantum field theory. For that purpose various methods such as regularization techniques, the schwinger proper time and the effective action will be explored. Secondly, it has been known for a long time that radiative corrections to the Casimir force can be computed within the framework of the low-energy Quantum Electrodynamics. There are two such contributions known as the Uehling and Euler-Heisenberg corrections.

These will also be discussed briefly.

Keywords: casimir force, van der waals, effective action, schwinger proper time, regularization methods, radiative corrections

ÖZ

BİR HALKA SEVİYESİNDE CASİMİR KUVVETİNİN ARAŞTIRILMASI

Yalçın, Nergis Nevra
Yüksek Lisans, Fizik Bölümü
Tez Yöneticisi: Prof. Dr. İsmail Turan

Şubat 2021 , 44 sayfa

Casimir kuvveti ilk olarak 1948’de Hendrik Casimir tarafından keşfedildi ve ilk olarak Lamoreaux *et al.* tarafından, başarılı ölçümleri neredeyse elli yıl süren, hesaplanan iki nötr iletken paralel plaka geometrisi için önerilen fiziksel bir etkidir. Temel olarak, kuantum vakumunun kendisinden kaynaklanan bir kuvvetin varlığını tanımlar. Yıllardır, kuantum elektrodinamiği denen teoremin deneysel sonuçlarla uyumu üzerinde çalışmalar yoğunlaşmıştır. Yıllar geçtikçe konu muazzam bir şekilde büyüdü ve hatta mühendislik kadar fizikte de disiplinler arası çalışmaların konusu haline geldi. Lamoreaux’nun kontrol altına alınan deneysel hatalarla yaptığı ölçümden sonra, birçok çalışma bundan ilham aldı ve daha sonra daha verimli olduğu kanıtlanmış küresel ve silindirik yüzeyler dahil olmak üzere farklı geometrileri içerecek şekilde genişletildi. Tezin temel amacı iki yönlüdür. İlk olarak, kuantum alan teorisini kullanarak casimir kuvvetinin kökenini en temel düzeyde anlamayı hedefliyoruz. Bu amaçla, düzenleme teknikleri, schwinger uygun zaman ve etkili eylem gibi çeşitli yöntemler araştırılacaktır. İkinci olarak, Casimir kuvvetine yönelik ışınım düzeltmelerinin düşük enerjili kuantum elektrodinamiği çerçevesinde hesaplanabileceği uzun zamandır bilinmektedir. Uehling ve Euler-Heisenberg düzeltmeleri olarak bilinen bu tür iki katkı

vardır. Bunlar da kısaca tartıřılacaktır.

Anahtar Kelimeler: casimir kuvveti, van der waals, etkin eylem metodu, schwinger
özgün zaman, düzenleme metodları, ışınımlı düzeltmeler

To Tarçın, Kar and Frida

ACKNOWLEDGMENTS

It is with sincere gratitude that I acknowledge the support and help of my supervisor Prof.Dr. İsmail Turan without whom this thesis would not be possible. It was always an honor and joy to work with him. It was also very important for me that he supported me not only in my studies but in my difficult times outside them as well.

I thank Meral Çelebi for his unconditional love, unending support and most importantly for always being by my side. I am glad you are my mother.

Thanks to my sister Melda Akalın for her support and attention ever since I started my studies here at METU.

Thank you very much to my high school friends Büşra Girgin, Hazal Tuna Berber, and Özge Bahadır for not leaving me alone for years. I am very lucky to have such friends in my life. I know we already promised to celebrate bigger.

Thank you to my dear friend Cansu Ceylan, whom I cried while laughing at the same time with for sharing my excitement.

Thank you Merve Soy for always guiding me you with your thoughts and approaches.

Even though our undergraduate life is over, I would like to thank Gilda Afshari, Hazal Doğaroğlu, and Merve Akkaya, whom I know keep me in their minds.

I thank each member of ele41, especially Arif Ozan Kızıldağ, Ayda Sehlikoğlu, Balam Kaynakçı, Buğra Yavuz, Ferdi Isıkay, Yaşar Okudan for their support.

I also thanks to my zumba family members Aytuğ Meriç(aytus), Ceren Erzin(sahmeran), Damla Özkan(wuhukenks), Gizem Özbek(coffeemate), Hilal Demir(sis), Nilya Bengül(nilyakus) and my dear Şule Akdoğan for being crazy with me. Dancing with you has always been a pleasure.

I would like to thank my friends Alim Yolalmaz, Deniz Bender and Şahin Kürekci

for nice conversations, especially in QC.

I would like to thank our dear secretary, Gülşen Özdemir Parlak, for answering all my questions throughout my undergraduate and graduate life without getting tired.

I owe a special thanks to my beloved husband Fırat Yalçın for being with me all the time when I needed it and for never losing his support and love.

I would also like to thank everyone who believes that all living things in the world have the right to live. #hayvanhaklarıyasatr

This work is financially supported by TÜBİTAK (The Science and Technological Research Council of Turkey)(Grant no:118F390).

TABLE OF CONTENTS

ABSTRACT	v
ÖZ	vii
ACKNOWLEDGMENTS	x
TABLE OF CONTENTS	xii
LIST OF TABLES	xiv
LIST OF FIGURES	xv
LIST OF ABBREVIATIONS	xvi
LIST OF SYMBOLS	xviii
CHAPTERS	
1 INTRODUCTION	1
1.1 Motivation	1
1.2 Introduction	1
2 EXPERIMENTAL PART OF CASIMIR EFFECT	5
3 CALCULATION OF CASIMIR FORCE BETWEEN PARALLEL PLATES	9
4 REGULARIZATION METHODS	13
4.1 Regularization Methods	13
4.1.1 Dimensional Regularization Method	13
4.1.2 Zeta Regularization Method	15

5	CALCULATION OF CASIMIR FORCE USING EFFECTIVE ACTION METHOD	19
5.1	Calculation of Casimir Force Using Effective Action Method	19
5.1.1	Effective Action	19
5.1.2	The Schwinger's Proper Time Method	20
5.1.3	The Feynman's Path Integral Method	24
5.2	Radiative Corrections to the Casimir Force	29
6	CONCLUSION	37
	REFERENCES	39
	APPENDICES	
A	DERIVATION OF \mathcal{D}^2	43

LIST OF TABLES

TABLES

Table 2.1 The geometries of experimental setups used in Casimir force measurement from past to present, the shortest distances reached and measurement precision are given.	7
---	---

LIST OF FIGURES

FIGURES

Figure 2.1	Casimir Force vs. Plate Separation graph	6
Figure 5.1	In the panel (a), the one-loop Feynman diagram responsible for the Uehling term before the electron field is integrated out is shown. In the panel (b), the electron loop is shrunk to a point.	30
Figure 5.2	In the panel (a), the Uehling diagram contributing the vacuum energy at the $\mathcal{O}(\alpha_{em})$ order is shown, obtained from from the panel (a) of Fig. 5.1 by connecting the external photon lines with each other. In the panel (b), the same but this time by using the the panel (b) of Fig. 5.1.	30
Figure 5.3	In the panel (a), the one-loop Feynman diagram responsible for the Euler-Heisenberg term before the electron field is integrated out is shown. In the panel (b), the electron box is shrunk to a point.	31
Figure 5.4	This is the Euler-Heisenberg diagram contributing the vacuum energy at the $\mathcal{O}(\alpha_{em}^2)$ order. Indeed this is obtained from the panel (b) of Fig. 5.3 by connecting the external photon lines with each other. . . .	31

LIST OF ABBREVIATIONS

ABBREVIATIONS

EAM	Effective Action Method
SM	Standard Model
QED	Quantum Electrodynamics

LIST OF SYMBOLS

SYMBOLS

α : Alpha

\approx : Approximation

β : Beta

δ : Delta

det : Determinant

ϵ : Epsilon

γ and Γ : Gamma

\int : Integral

∞ : Infinity

λ : Lambda

μ : Mu

ν : Nu

ω and Ω : Omega

\parallel : Parallel

ϕ : Phi

π : Pi

\prod : Product

ψ : Psi

σ : Sigma

$\sqrt{\quad}$: square

\sum : Summation

Tr : Trace

ε : Varepsilon

ζ : Zeta

CHAPTER 1

INTRODUCTION

1.1 Motivation

Our first aim is to achieve in this thesis to understand the so-called Casimir effect as a one-loop effect by using quantum field theory. Before this calculation, we are focused on derivation and calculation of Casimir effect. We carried on this calculation by using some regularization methods. In addition to this, we compared the results with theoretical and experimental findings. Furthermore we also explained the use of the effective action and Schwinger proper time methods for the calculation of the Casimir force between two parallel conducting plates.

1.2 Introduction

Many inventions have affected the progress of Physics. Some still have an important effect on lots of physical configurations. Casimir effect is one of them. Today, they are various different views on the measurement and results of this force. But, one point is common : the relation between the Casimir force and the Van der Waals force, is used for understanding of the nature of the force(s).

Van der Waals has interested in critical temperatures which are related to Andrews' experiments(1869).Then, he realized that we have to calculate volumes of molecules and the intermolecular forces (called Van der Waals forces in general) to understand relationship between the pressure, temperature and volume of liquids and gases. After that, Van der Waals found in 1873 that significant improvements could be effected by including a finite size of the molecules and weak forces between the molecules. These

forces were introduced in a completely ad-hoc manner by placing two parameters in the equation of state.

Shortly, Van der Waals force examines interactions, which depends on distances between atoms or molecules. In addition to this information, these forces include attractions and repulsions between surfaces, atoms, molecules. In this way, Dutch scientist Johannes Diderik van der Waals explained intermolecular forces in 1873. After that London (1930) gave an explanation of intermolecular forces with a new phenomena, which is called London forces. According to London, these forces are weak intermolecular forces, which come out the interactive forces between temporary (instantaneous) multipoles in molecules. While the London dispersion force between individual atoms and molecules is quite weak and decreases quickly with separation (r) like r^{-6} . [1] [2]

After this, Casimir and Polder also did some research about intermolecular forces and they calculated relativistic correction (they added retardation) for them. Casimir and Polder introduced a term which called retardation, and they wrote a paper about influence of retardation on Van der Waals forces. After this, they found that the interaction between molecules goes like r^{-7} at large distance. This can be easily understood by dimensional argument.

Like Van der Waals force, Casimir one also acts between closely spaced, uncharged surfaces. They both are pure quantum origin whose root goes back to the zero-point energy. They do not spawn the action of electric or magnetic fields because their mean values are zero. Due to field dispersions, they are generally called by a generic name of dispersion forces.[1] Actually, Casimir and Van der Waals forces are not distinct ones. Van der Waals force is subdivision of dispersion force, which affects at very short distances. On the other hand, Casimir forces are also dispersion forces but they are effective at larger distances, where the effect of the relativistic retardation should be taken into account.[2]

Moreover, after Casimir and Polder is result, Bohr suggested to Casimir that it should be somehow related to vacuum energy. Thus, Casimir did his explanation based on vacuum energy instead of van der Waals. In 1948, he performed the theoretical calculation based on vacuum energy when the molecules are replaced by two perfectly

conducting parallel plates. That is the simplest way to show and calculate the Casimir force.

After this information, to evaluate our hypothesis we also calculated the Casimir effect between two perfectly conducting parallel plates. The Casimir effect brings an explanation about the that attraction between atoms or molecules. Like Casimir, we also found that electric field is zero because of plates being electrically neutral. On the other hand, the square of the magnetic and electric fields are not equal to zero. So, we can clearly say that the expectation value of the energy is not zero and we initially understand that there is measurable force between these plates. We cannot reach precise information about the sign of the force. After doing some calculation, we get

$$F = -\frac{\pi^2}{240a^4}\hbar c \quad (1.1)$$

where a is the distance between plates.

Having this result at hand, many scientists examined the consistency between the theory and experiment. However, based on the studies of Lamoreaux and his colleagues, it was revealed that the experimental data and the theory are compatible with each other. Actually, the experimental studies are not limited to Lamoreaux. Many others, like Sparnaay and Mohideen, have basically made some experimental contributions on parallel plate geometry. After years, to get better precision, scientists made some modifications in geometry and surfaces.[3] [4] [5] The theoretical part, on the other hand, is much harder than thought because Casimir energies are shown to be infinite. However, energy differences are quite often infinite. Because of this, one has to use regularization methods to calculate the Casimir force. Although there are many regularization methods, we will use two of them, namely the Dimensional and Zeta Regularization Methods.

Over the years, there has been tremendous developments in both experimental and theoretical efforts in the Casimir effect business. Different experimental and theoretical techniques have been implemented to achieve a better precision in measurements or better understanding in calculations. In theoretical approaches, it is quite common

to use a simplifying analogy (like using a scalar field etc) to carry out the calculation. Despite these means being as reputable as they are, one may still look for a quantum field theory level (namely quantum electrodynamics) understanding of the Casimir force. This might serve two purposes here. One is to show explicitly the connection between the vacuum energy (rather than the zero-point energy directly) and the Casimir force. The other one is to find a well defined way to calculate the Casimir force if the vacuum is modified, say, with the presence of some new particles.

To achieve the first purpose we will devise the so-called effective action method after explaining its basics. We can clearly say that the action plays a very important role in classical and quantum physics. Effective action denoted by Γ and it refers to a functional of actions. In the classical approach, S is named as action of full energy and it differs from Γ . Γ has fewer fields and it is nonrenormalizable. These features make it easy for us to calculate.

About the second purpose, we are interested in radiative corrections to the Casimir force. Concentrating on the effective QED by assuming energies is one way to calculate radiative correction. Using order α and α^2 one can express Uehling and Euler-Heisenberg correction. It is also possible to access these corrections via Feynman diagrams. Energy density correction $\Delta\mathcal{E}$ due to Euler-Heisenberg interaction, $\Delta\mathcal{E} = -\mathcal{L}_{EH}$, that is, the contribution to Casimir energy arises from this interaction.

CHAPTER 2

EXPERIMENTAL PART OF CASIMIR EFFECT

In 1958, Sparnaay not only managed to measure the Casimir force between two parallel plates but he also was the first person to get a decent agreement between the theory and the experiment.

After Sparnaay's experiment, Lamoreaux and his student worked on the measuring the Casimir force (1996). They used a torsion pendulum because it is very sensitive for very feable forces. In this experiment, they measured the Casimir force between a flat gold plate and a gold-plated spherical lens [3]. The amount of force required to keep pendulum at the same angle was measured while plate and lens were brought together very closely. To use spherical lens surface in terms of the second plate, Lamoreaux applied the proximity force approximation and their findings were very satisfactory.

Late 90s, Mohideen and Roy are also interested Casimir force using the sphere-plate set up. In the experiment, the force was created by bringing gold plated saphire optically flat surface closer to a sphere and observing the motion of the end of the cantilever [4]. Then, they observed angle of reflection and measured the force by using this method. They got results with only 1% disagreement with theory in 1998. Bell Labs, an approach similar to Mohideen with a plate-sphere geometry was used in 2001.

Decca *et al.* measured the force between dissimilar metals with a plate-sphere geometry as well. The results agree to theoretical ones with less than 1% discrepancy when the range is between 0.2 to 0.5 microns. However, at larger distances (0.5 to 2 microns) they observed bigger discrepancy.[6] One possible source of this discrep-

ancy were thought to be related to incomplete characterisation of the metal surfaces (2003).

In 2004, Iannuzzi and his colleagues also used an experimental set up similar to the Bell Labs system which measured the displacement of the cantilever using capacitive electrodes on and below the plate.[7] Showing a change in optical properties upon exposure to hydrogen.

These experimental developments took a place thanks to Sparnaay, as we have mentioned before. Hence, the casimir force per unit area is depicted as a function of the plate separation in Figure 2.1 and the experimental data are taken from the Sparnaay's paper [[5]]. The theory and data are in good agreement.

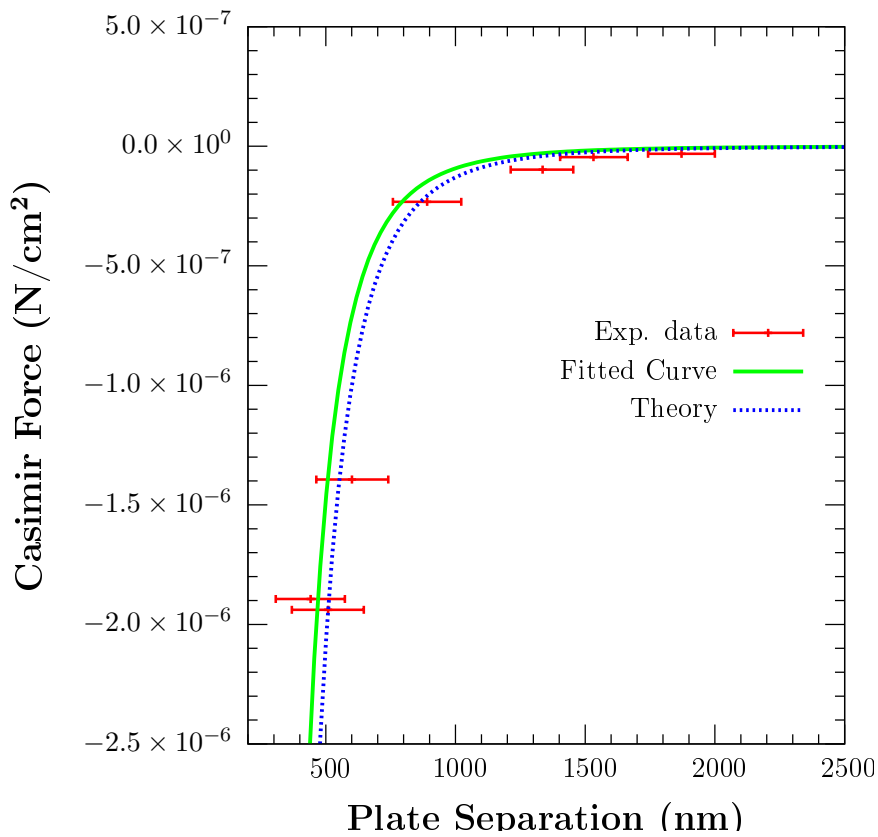


Figure 2.1: Casimir Force vs. Plate Separation graph

Table 2.1: The geometries of experimental setups used in Casimir force measurement from past to present, the shortest distances reached and measurement precision are given.

Casimir Force Experiments List				
Year	Geometry	Range(μm)	Accuracy(%)	Source
1958	plane-plane	0.3÷2.5	100	[5]
1978	plane-sphere	0.13÷0.67	25	[8]
1996	plane-sphere	0.6 ÷12.3	5	[3]
1998	plane-sphere	0.1÷0.9	1	[4]
2000	crossed cylinders	0.02÷0.1	1	[9]
2001	plane-sphere	0.08÷1.0	1	[10]
2002	plane-sphere	0.5÷3.0	15	[11]
2003	plane-sphere	0.2÷2.0	1	[6]
2004	plane-sphere	0.3÷2.5		[7]
2005	plane-plane(Au coated)	0.17÷0.42	5	[12]
2006	sphere-plane	0.1÷0.4	5	[13]
2008	sphere-plane	0.2÷0.5	10	[14]
2009	plate-plate(Plasma-like)	0.16÷0.75	5	[15]
2009	plate-plate(Drude Model)	0.21÷0.62	1	[16]
2011	plate-plate	0.01÷1	5-7	[17]
2012	plate-sphere	0.1÷20		[18]
2012	plate-sphere&plate-plate	0.1÷0.7	3-33	[19]
2016	Au&Ni coated spheres	0.2÷0.7		[20]
2017	Au sphere-plate	0.2÷4	≈ 1	[21]
2018	Au surfaces (liquid & gas)	0.05÷0.3		[22]
2019	super conducting plates	0.06÷0.2	5.1	[23]

CHAPTER 3

CALCULATION OF CASIMIR FORCE BETWEEN PARALLEL PLATES

As I mentioned before Casimir effect is generally used for showing attraction between atoms or molecules. Dutch physicists Hendrik Casimir and Dirk Polder worked on the force between two polarizable atoms. They used two neutral conducting parallel plates to understand and calculate this force. The electric field is zero since the plates are neutral. But, the same is not true of the square of electric and magnetic fields. So, the expectation value of the energy is not equal to zero.[24] We can understand that there is a measurable force on the plates. When making these calculations, if the dimensional length is called L and the distance between the plates is called, an expression $a \ll L$ can be used. Otherwise, these plates at very close range behave infinitely large.

Due to the conductivity of the plates, the wave field vector occurs perpendicular to the surface of the plates. Therefore, vectors can only have discrete values along the perpendicular direction. If we consider the direction perpendicular to the plates as z , the wave field vector k becomes k_z in this direction ($k_z = \frac{n\pi}{a}$). In this system, we call $E(a)$ the energy that the plates have at distance a and as a result we understand that the work done to remove the plates up to δa is connected with the vacuum energy. The calculation of this vacuum energy is related to the definition of "half quanta" mentioned by Plank in 1911.[25] According to Plank, the energy levels in harmonic oscillator are written as

$$E_n = \frac{\hbar\omega}{2} \quad (3.1)$$

Since this basic energy value cannot be measured precisely, the quantum field theory

describes energy as

$$E_0 = \sum_j \frac{1}{2} \hbar \omega_j \quad (3.2)$$

The number j represents quantum numbers of the field modes. In electromagnetic field, a wave vector has two transverse polarization states so we consider this situation for calculation of Casimir force and if we write energy accordingly

$$E(a) = \sum_j \frac{1}{2} \hbar \omega_j = \frac{\hbar c}{2} \sum_j |k_j| = \frac{\hbar c}{2} \int L^2 \frac{d^2 k_\perp}{(2\pi)^2} \left[k_\perp + 2 \sum_{n=1}^{\infty} \left(k_\perp^2 + \frac{n^2 \pi^2}{a^2} \right)^{\frac{1}{2}} \right] \quad (3.3)$$

where $k_\perp = \sqrt{k_x^2 + k_y^2}$. Considering zero-point energy level, we integrate over k_\parallel and the result is calculated infinite as we expected. To clarify this situation, if the same calculation is repeated for the absence of plates, in this case, since there will be no cuts in the z direction, all three dimensions should be integrated. Later, the variable k_z can be converted to n for some advantage.

$$E_0 = \frac{\hbar c}{2} \int L^2 \frac{d^2 k_\perp}{(2\pi)^2} \int_{-\infty}^{\infty} \frac{dk_z}{2\pi} 2\sqrt{k_\perp^2 + k_z^2} = \frac{\hbar c}{2} \int L^2 \frac{d^2 k_\perp}{(2\pi)^2} \int_0^{\infty} dn \sqrt{k_\perp^2 + \frac{n^2 \pi^2}{a^2}} \quad (3.4)$$

We can clearly state that E_0 also equal to infinity for this situation. Since E_0 is related to the energy of the vacuum, regardless of the presence of plates, it is significant to look at the energy difference between the post-plate state and the pre-state, and if we calculate this difference per unit surface area. Then we get

$$\mathcal{E} = \frac{E(d) - E_0}{L^2} = \frac{\hbar c}{2\pi} \int_0^{\infty} k dk \left(\frac{k}{2} + \sum_{n=1}^{\infty} \sqrt{k^2 + \frac{n^2 \pi^2}{d^2}} - \int_0^{\infty} dn \sqrt{k^2 + \frac{n^2 \pi^2}{a^2}} \right) \quad (3.5)$$

Although energy is convergent, it is still divergent for large values of k . Therefore, if we integrate with the cutting method, which is one of the regularization methods

that will be discussed in more detail in the following sections, it is only written in the range where k_{max} .

$$\mathcal{E} = \hbar c \frac{\pi^2}{4a^3} \int_0^\infty ds \left[\frac{\sqrt{s}}{2} f\left(\frac{\pi}{a}\sqrt{s}\right) + \sum_{n=1}^\infty \sqrt{s+n^2} f\left(\frac{\pi}{a}\sqrt{s+n^2}\right) - \int_0^\infty dn \sqrt{s+n^2} f\left(\frac{\pi}{a}\sqrt{s+n^2}\right) \right] \quad (3.6)$$

Here it is defined as $s = d^2 k^2 / \pi^2$. To simplify this equation, if a new $F(n)$ is created as below.

$$F(n) = \int_0^\infty ds \sqrt{s+n^2} f\left(\frac{\pi}{a}\sqrt{s+n^2}\right) \quad (3.7)$$

If the equation is expressed again in terms of pressure and $F(n)$

$$\mathcal{E} = \hbar c \frac{\pi^2}{4a^3} \left[\frac{1}{2} F(0) + \sum_{n=1}^\infty F(n) - \int_0^\infty dn F(n) \right] \quad (3.8)$$

Bernouli numbers are obtained in this equation with the help of Euler-Maclaruin addition.

$$F(n) = \int_{n^2}^\infty ds \sqrt{s} \left(f\left(\frac{\pi}{a}\sqrt{s}\right) \right), \quad F'(n) = -2n^2 f\left(\frac{n\pi}{a}\right) \quad (3.9)$$

According to this information, all values except $F'''(0)$ give zero for $n = 0$.

$$\mathcal{E} = -\frac{\pi^2}{720} \frac{\hbar c}{a^3} \quad (3.10)$$

After this result, by using the relation ε with the force, we get the following expression for the Casimir force between parallel plates.

$$F = -\frac{\partial \mathcal{E}}{\partial a} = -\frac{\pi^2}{240} \frac{\hbar c}{a^4} \quad (3.11)$$

where a is called distance between two polarizable plates. Using this result, we clearly understand that our result for pressure and force is finite and they are compatible with experiments. In the next section we will look at the results that systematize reaching this conclusion.

CHAPTER 4

REGULARIZATION METHODS

4.1 Regularization Methods

4.1.1 Dimensional Regularization Method

For simplicity, we use massless scalar field ϕ confined between two parallel plates which are separated by distance a . The field has Dirichlet boundary conditions on the neutral plates. The conditions are

$$\phi(z = 0) = \phi(z = a) = 0 \quad (4.1)$$

We know that energy can be written for over all modes

$$\begin{aligned} \varepsilon &= \frac{1}{2} \sum_{\text{modes}} \hbar\omega \\ &= \frac{1}{2} \sum_{n=1}^{\infty} \int \frac{d^D \vec{k}}{4\pi^2} \sqrt{\vec{k}^2 + \frac{n^2\pi^2}{a^2}} \end{aligned} \quad (4.2)$$

where we take $\hbar = c = 1$. Moreover, n is positive integer and \vec{k} is the transverse momentum. We let the transverse dimension be D , which we will subsequently treat as a continuous, complex variable. We also use the Schwinger proper-time representation for this regularization.[26] We can write

$$\varepsilon = \frac{1}{2} \sum_n \int \frac{d^D k}{(2\pi)^D} \int_0^\infty \frac{dt}{t} t^{-1/2} e^{-t(k^2 + n^2\pi^2/a^2)} \frac{1}{\Gamma(-\frac{1}{2})} \quad (4.3)$$

To get this integral, we use the Euler representation for the gamma function

$$\int_0^{\infty} t^n e^{-at} dt = \frac{\Gamma(n+1)}{a^{n+1}} \rightarrow a^{-(n+1)} = \frac{1}{\Gamma(n+1)} \int_0^{\infty} t^n e^{-at} dt \quad (4.4)$$

After that, we take this Gaussian integration sum over k and get

$$\varepsilon = \frac{-1}{4\sqrt{\pi}} \frac{1}{(4\pi)^{\frac{D}{2}}} \sum_0^{\infty} \frac{dt}{t} t^{\frac{-1}{2} - \frac{D}{2}} e^{-tn^2\pi^2/a^2} \quad (4.5)$$

Using Euler representation and definition of Riemann zeta function:

$$\varepsilon = \frac{-1}{4\sqrt{\pi}} \frac{1}{(4\pi)^{\frac{D}{2}}} \frac{\pi^{D+1}}{a^{D+1}} \Gamma\left(\frac{-D+1}{2}\right) \zeta(-D-1) \quad (4.6)$$

D is an odd integer now and we can use reflection property of gamma function to rewrite equation (4.5) as

$$\varepsilon = \frac{-1}{2^{D+2}} \frac{1}{\pi^{D/2+1}} \frac{1}{a^{D+1}} \Gamma(1+D/2) \zeta(2+D) \quad (4.7)$$

We know that this formulation is only valid for $\text{Re } D < -1$ and zeta function is only suitable if $\text{Re } D < -2$. Thus, we calculate general result for this equation at $D = 2$ and it gives

$$\epsilon = \frac{-\pi^2}{1440} \frac{1}{a^3} \quad (4.8)$$

where $\zeta(4) = \frac{\pi^4}{90}$. Using force and energy relation

$$F = \frac{-\partial\epsilon}{\partial a} = \frac{-\pi^2}{480} \frac{1}{a^4} \quad (4.9)$$

This result gives us Casimir force due to scalar field. The force between two parallel plates as a result of electromagnetic fluctuations may be calculated by multiplying the

result by 2 due to two polarization states of the photon and this gives

$$F_{em} = \frac{-\pi^2}{240} \frac{1}{a^4} \quad (4.10)$$

4.1.2 Zeta Regularization Method

Before calculating Casimir force with using zeta regulator, first we describe what zeta function is. The Riemann Zeta function $\zeta(s)$, which is a function of a complex variable s [27].

$$\sum_{n=1}^{\infty} \frac{1}{n^s} \quad (4.11)$$

This summation is convergent for all complex values of s when $\text{Re } s > 1$ and this situation defines $\zeta(s)$ as the analytic continuation. Riemann used this information and formulated this for non-trivial zeros of zeta functions in 1859 [27]. After years, Robert Seeley's work showed that we can define a determinant using zeta function regularization. In 1971, Ray and Singer used Seeley's theory in their paper to define determinant of a positive self-adjoint operator K [28].

$$\zeta_K(s) = \text{Tr}(K^{-s}) \quad (4.12)$$

The method defines also the (possibly divergent) infinite product as

$$\prod_{n=1}^{\infty} a_n = \exp[-\zeta_{K'}(0)] \quad (4.13)$$

Using some information about traces, we get

$$\zeta_K(s) = \text{Tr} K^{-s} = \sum_j \lambda_j^{-s}, \quad \text{Re } s > \frac{n}{M} \equiv \frac{\dim A}{\text{ord} K} \quad (4.14)$$

where n is dimensional vector and M is dimensional manifold. After that, we use

definition of zeta function and take derivative at $s = 0$.

$$\zeta'_K(0) = - \sum_{i \in \epsilon} \ln \lambda_i \quad (4.15)$$

and from definition of the determinant of K :

$$\det_\zeta = \exp[-\zeta'_K(0)] \quad (4.16)$$

For multiplicative (or non commutative) anomaly, the determinant is

$$\ln \left[\frac{\det_\zeta(AB)}{\det_\zeta A \det_\zeta B} \right] = -\zeta_A B'(0) + \zeta'_A(0) + \zeta'_B(0) \quad (4.17)$$

Using this information, we also calculate Hamiltonian for 3D system and get

$$H = \int \frac{d^3k}{(2\pi)^3} \omega_k (a_k^\dagger a_k + 1/2) \quad (4.18)$$

Then, we can write energy as

$$E = \langle 0 | \hat{H} | 0 \rangle = \int \frac{d^3k}{(2\pi)^3} \frac{\omega_k}{2} \approx \frac{1}{4\pi^2} \int k^3 dk \quad (4.19)$$

This gives us divergent result. To get finite result, we use zeta regulator here. Moreover, using summing over method, the expectation value of energy can be written as

$$\langle E \rangle = \frac{1}{2} \sum_n E_n \quad (4.20)$$

where n gives us all possible values for energy. Like dimensional method, we try to calculate Casimir energy between two conducting parallel plates at distance a apart. For simplicity, we consider that our system involves massless scalar field. We assume

that parallel plates lie in the xy - plane. Then, the standing waves are

$$\varphi_k(x, t) = e^{-i\omega_k t} e^{ik_x x + ik_y y} \sin(k_k z) \quad (4.21)$$

where φ is the electric component and k_k is equal to $\frac{n\pi}{a}$. ω_k is the energy of this wave and given as

$$\omega_k = \sqrt{(k_x)^2 + (k_y)^2 + \frac{n^2 \pi^2}{a^2}} \quad (4.22)$$

Inserting equation (4.22) into equation (4.20) and get

$$\langle E \rangle = \frac{1}{2} \sum \frac{dk_x dk_y}{(2\pi)^2} \sum_{n=1}^{\infty} A \omega_k \quad (4.23)$$

where A represents the area of each metal plate and factor of two is introduced for the two possible polarizations of the wave. We introduce the zeta regulator to make the expression finite and get

$$\langle E(s) \rangle = \int \frac{dk_x dk_y}{(2\pi)^2} \sum_{n=1}^{\infty} \omega_k |\omega_k|^{-s} \quad (4.24)$$

This integral can be finite if $s > 3$.

$$\begin{aligned} \frac{\langle E(s) \rangle}{A} &= \int \frac{dk_x dk_y}{(2\pi)^2} \sum_{n=1}^{\infty} \sqrt{(k_x)^2 + (k_y)^2 + \frac{n^2 \pi^2}{a^2}} \left| (k_x)^2 + (k_y)^2 + \frac{n^2 \pi^2}{a^2} \right|^{-\frac{s}{2}} \\ &= \frac{1}{4\pi^2} \int dk_x dk_y \sum_{n=1}^{\infty} \left| (k_x)^2 + (k_y)^2 + \frac{n^2 \pi^2}{a^2} \right|^{\frac{1-s}{2}} \end{aligned} \quad (4.25)$$

Now, using polar coordinates, we rewrite the equation above:

$$\begin{aligned}
\frac{\langle E \rangle}{A} &= \frac{1}{4\pi^2} \sum_n \int_0^\infty \int_0^{2\pi} k dk d\theta \left| k^2 + \frac{n^2 \pi^2}{a^2} \right|^{\frac{1-s}{2}} \\
&= \frac{1}{4\pi^2} 2\pi \sum_n \int_0^\infty dk k \left| k^2 + \frac{n^2 \pi^2}{a^2} \right|^{\frac{1-s}{2}} \\
&= \frac{1}{2\pi} \sum_n \frac{n^2 \pi^{\frac{3-s}{2}}}{a^2} \frac{\pi^{3-s}}{s-3} \\
&= \frac{-1}{2a^{3-s}} \frac{\pi^{2-s}}{3-s} \sum_n |n|^{3-s}
\end{aligned} \tag{4.26}$$

In the last line above, the Riemann zeta function is obtained and taking the $s = 0$ limit, one gets.

$$\begin{aligned}
\frac{\langle E \rangle}{A} &= \lim_{s \rightarrow 0} \frac{\langle E \rangle}{A} \\
&= \frac{-1}{2a^3} \frac{\pi^3}{3} \zeta(-3) \\
&= \frac{-\pi^2}{6a^3} \frac{1}{120} \\
&= \frac{-\pi^2}{720a^3}
\end{aligned} \tag{4.27}$$

where $\zeta(-3) = \frac{1}{120}$ is used. The Casimir force per unit area is

$$\begin{aligned}
\frac{F}{A} &= -\frac{1}{A} \frac{\partial \langle E \rangle}{\partial a} \\
&= -\frac{\pi^2}{240a^4}
\end{aligned} \tag{4.28}$$

CHAPTER 5

CALCULATION OF CASIMIR FORCE USING EFFECTIVE ACTION METHOD

5.1 Calculation of Casimir Force Using Effective Action Method

Generally people used scalar field or electromagnetic field for Casimir force calculations. Although these methods are used frequently, effective action method is basically used for force calculation.

5.1.1 Effective Action

Effective action generally used for fields and converts equations of motion into motion with the principle of motion. However, we cannot apply this to quantum field theory. Because, in quantum field theory, all possible moves are summed on a path integral and if use effective action instead of action, motion actions can only be obtained when the active action is fixed. Effective action is represented by Γ and obtained as $\Gamma = \int d^4x \mathcal{L}$. In this formula, \mathcal{L} is called effective Lagrangian. [29] [30] In QED system, we can write effective action for massive fermion¹

$$\int \mathcal{D}A \exp(i\Gamma[A_\mu]) \equiv \int \mathcal{D}A \mathcal{D}\bar{\psi} \mathcal{D}\psi \exp \left[i \int d^4x \left(-\frac{1}{4} F_{\mu\nu}^2 + \bar{\psi}(i\mathcal{D} - m)\psi \right) \right] \quad (5.1)$$

If the fixed electromagnetic field A_μ is \mathcal{L} , it denotes Euler-Heisenberg Lagrangian. Effective action method can be obtained and used in different ways. We will try to

¹ In most part of this chapter, we closely follow the book by Schwartz [31].

obtain EAM using this method, Schwinger proper time method and Feynman's path integral method.

5.1.2 The Schwinger's Proper Time Method

If we consider Schwinger's method first, this method helps to create a propagator to obtain other fields. It can be mathematically expressed as:

$$\frac{i}{A + i\varepsilon} = \int_0^\infty ds e^{is(A+i\varepsilon)} \quad (5.2)$$

Let us discuss the scalar and spinor cases separately.

- *The scalar case:*

The Feynman propagator for the scalar case is described mathematically as

$$\begin{aligned} D_F(x, y) &= \int \frac{d^4k}{(2\pi)^4} e^{ik(x-y)} \frac{i}{k^2 - m^2 + i\varepsilon} \\ &= \int \frac{d^4k}{(2\pi)^4} e^{ik(x-y)} \int_0^\infty ds e^{is(k^2 - m^2 + i\varepsilon)} \end{aligned} \quad (5.3)$$

Integral is gaussian and we put $A = -2isg^{\mu\nu}$ in our configuration

$$D_F(x, y) = \frac{-i}{16\pi^2} \int_0^\infty \frac{ds}{s^2} e^{-i \left[\frac{(x-y)^2}{4s} + sm^2 - i\varepsilon s \right]} \quad (5.4)$$

Massless situation gives us position-space Feynmann propagator. With knowledge of non-relativistic quantum mechanics and Hilbert space, $\langle k|x \rangle (x = e^{ikx})$ and using this analogy

$$\begin{aligned} D_F(x, y) &= \int \frac{d^4k}{(2\pi)^4} \langle y|k \rangle \int_0^\infty ds e^{is(k^2 - m^2 + i\varepsilon)} \langle k|x \rangle \\ D_F(x, y) &= \int_0^\infty ds e^{-s\varepsilon} e^{-ism^2} \langle y|e^{-is\hat{H}}|x \rangle \\ &\equiv \int_0^\infty ds e^{-s\varepsilon} e^{-ism^2} \langle y; 0|x; s \rangle \end{aligned} \quad (5.5)$$

where $|x; s \rangle = e^{-is\hat{H}}|x \rangle$ is defined and $\hat{H} = -\hat{p}^2$ is assumed.

The Feynman propagator D_F can also be derived by using the Green's function

$$\hat{G} \equiv \frac{i}{\hat{k}^2 - m^2 + i\varepsilon}$$

$$\begin{aligned} D_F(x, y) &= \int \frac{d^4k}{(2\pi)^4} e^{ik(x-y)} \frac{i}{k^2 - m^2 + i\varepsilon} \\ &= \int \frac{d^4k}{(2\pi)^4} \langle y|k\rangle \langle k| \frac{i}{\hat{k}^2 - m^2 + i\varepsilon} |x\rangle \\ &= \langle y|\hat{G}|x\rangle \end{aligned} \tag{5.6}$$

$$= \int_0^\infty ds e^{-s\varepsilon} e^{-ism^2} \langle y|e^{-i\hat{H}s}|x\rangle \tag{5.7}$$

Now considering Lagrangian for scalar case,

$$\mathcal{L} = -\frac{1}{4}F_{\mu\nu}^2 - \phi^*(D^2 + m^2)\phi \tag{5.8}$$

where $D_\mu = \partial_\mu + ieA_\mu$.

As a step towards getting the effective Lagrangian, one needs to calculate the Green's function in the background of the electromagnetic field A_μ . It is defined as

$$G_A(x, y) = \langle A|T\phi(y)\phi^*(x)|A\rangle \tag{5.9}$$

Using $\partial_\mu \rightarrow -i\hat{k}_\mu$ we get

$$\hat{G}_A = \frac{i}{(\hat{k} - eA(\hat{x}))^2 - m^2 + i\varepsilon} \tag{5.10}$$

$$\begin{aligned} G_A(x, y) = \langle y|\hat{G}_A|x\rangle &= \langle y| \frac{i}{(\hat{k} - eA(\hat{x}))^2 - m^2 + i\varepsilon} |x\rangle \\ &= \int ds e^{-s\varepsilon} e^{-ism^2} \langle y|e^{-i\hat{H}s}|x\rangle \end{aligned} \tag{5.11}$$

This equation can be written in the case where $\hat{H} = -(\hat{k} - eA(\hat{x}))^2$. Here $G_A(x, y)$ shows the evolution of ϕ from x to y in s time.

The full Lagrangian in equation 5.8 can be transformed into an effective form by integrating over the complex scalar field. Even though this derivation is

possible to do with the Schwinger's method, we will leave it for later to do by using the Feynman's path integral which is much faster.

- *The spinor case:*

For the spinor case, we define $G_A(x, y)$ and the covariant derivative for the Dirac spinor.

$$G_A(x, y) = \langle A | T \psi(y) \bar{\psi}(x) | A \rangle$$

$$\mathcal{D}^2 = D_\mu^2 + \frac{e}{2} F_{\mu\nu} \sigma^{\mu\nu} \quad (5.12)$$

where the derivation of \mathcal{D}^2 is given in Appendix A. The term $F_{\mu\nu} \sigma^{\mu\nu}$ is the additional term in the case of spinor as compared to the scalar field. In the momentum space, an equation can be mentioned thanks to this value.

$$(\hat{k} - e\mathcal{A}(\hat{x}))^2 = (\hat{k} - eA(\hat{x}))^2 - \frac{e}{2} F_{\mu\nu}(\hat{x}) \sigma^{\mu\nu} \quad (5.13)$$

The spinor of the Green function is defined.

$$\hat{G}_A = \frac{i}{\hat{k} - e\mathcal{A}(\hat{x}) - m + i\varepsilon}$$

$$= (\hat{k} - e\mathcal{A}(\hat{x}) + m) \frac{i}{(\hat{k} - eA(\hat{x}))^2 - \frac{e}{2} F_{\mu\nu}(\hat{x}) \sigma^{\mu\nu} - m^2 + i\varepsilon} \quad (5.14)$$

Dirac spinor is found in here.

$$G_A(x, y) = \langle y | \frac{i}{\hat{k} - e\mathcal{A} - m + i\varepsilon} | x \rangle$$

$$= \int_0^\infty ds e^{-s\varepsilon} e^{-ism^2} \langle y | (\hat{k} - e\mathcal{A}(\hat{x}) + m) e^{-i\hat{H}s} | x \rangle \quad (5.15)$$

If we remember the effective action method from this situation, we know that we can do the movement actions in an integrated way using the method. We usually use this event by showing the tree level system. It is correct to configure the method according to a case where Lagrangian is minimum to show EAM. When we look at classical physics, this situation provides quite logical

results. According to quantum physics, to obtain this minimum value event, it is necessary to determine a field according to the expectation value [30].

$$\Phi \rightarrow \langle \Omega | \Phi | \Omega \rangle \quad (5.16)$$

Our priority is to show the corrected electromagnetic field and apply it in the field. $\Phi \rightarrow \langle A | \Phi | A \rangle$ is used instead of Φ . In an electron case, it is necessary to calculate the Lagrangian of the system.

$$\mathcal{L} = -\frac{1}{4}F_{\mu\nu}^2 + \bar{\psi}(i\partial - m)\psi - eA_\mu\bar{\psi}\gamma\psi \quad (5.17)$$

Equation is rewritten by using $J_A^\mu \equiv \langle A | \bar{\psi}(x)\gamma^\mu\psi(x) | A \rangle$.

$$\mathcal{L}_{eff} = -\frac{1}{4}F_{\mu\nu}^2 - eA_\mu J_A^\mu \quad (5.18)$$

Using Schwinger's original time theorem, J_A^μ is calculated and $A = 0$ is valid for the vacuum system. So J_0^μ should take the propagator as $G(x, y)$. Using this information, we obtain the following equation.

$$\begin{aligned} J_0^\mu(x) &= \langle \Omega | \bar{\psi}_{\dot{\alpha}}(x)\gamma_{\dot{\alpha}\alpha}^\mu\psi_\alpha(x) | \Omega \rangle = -Tr \left[\langle \Omega | \psi_\alpha(x)\bar{\psi}_{\dot{\alpha}}(x)\gamma_{\dot{\alpha}\beta}^\mu | \Omega \rangle \right] \\ &\equiv -Tr \langle x | \hat{G}\psi^\mu | x \rangle \end{aligned} \quad (5.19)$$

Using connection between \hat{G}_A and $J_A^\mu(x)$, J_A^μ is written like this:

$$\begin{aligned} J_A^\mu &= -Tr \left[\int_0^\infty ds e^{s\varepsilon} e^{-ism^2} \langle x | \gamma^\mu(\not{k} - e\mathcal{A} + m)e^{-i\hat{H}s} | x \rangle \right] \\ &= - \int_0^\infty ds e^{-s\varepsilon} e^{-ism^2} \langle x | Tr \left[\gamma^\mu(\not{k} - e\mathcal{A})e^{i((k-eA)^2 - \frac{\varepsilon}{2}\sigma_{\mu\nu}F^{\mu\nu})s} \right] | x \rangle \end{aligned} \quad (5.20)$$

From here we use that the odd number values of the γ matrices are zero and rewrite J_A^μ .

$$J_A^\mu = -\frac{i}{2e} \frac{\partial}{\partial A_\mu} \int_0^\infty \frac{ds}{s} e^{-s\varepsilon} e^{-ism^2} Tr \left[\langle x | e^{-i\hat{H}s} | x \rangle \right] \quad (5.21)$$

The right and left sides are integrated with respect to A_μ and add \mathcal{L}_{eff} to the equation

$$\mathcal{L}_{eff}^{ferm}(x) = -\frac{1}{4}F_{\mu\nu}^2(x) + \frac{i}{2} \int_0^\infty \frac{ds}{s} e^{-s\varepsilon} e^{-ism^2} \text{Tr} \left[\langle x | e^{-i\hat{H}s} | x \rangle \right] \quad (5.22)$$

where $\hat{H} = -(\hat{k}^\mu - eA^\mu(\hat{x}))^2 + \frac{e}{2}F_{\mu\nu}(\hat{x})\sigma^{\mu\nu}$ is defined for spinors.

5.1.3 The Feynman's Path Integral Method

As promised earlier, the effective Lagrangian of the complex scalar field can be found using the so-called Feynman path integral in an easier manner. Let us justify this. Obviously a similar calculation can be carried out for the fermion case as well.

For the scalar QED with the complex field ϕ , the Feynman path integral is written as follows.

$$\int \mathcal{D}A \exp(i\Gamma[A]) = \int \mathcal{D}A \mathcal{D}\phi \mathcal{D}\phi^* \exp \left[i \int d^4x \left(-\frac{1}{4}F_{\mu\nu}^2 - \phi^*(D^2 + m^2)\phi \right) \right] \quad (5.23)$$

In this case, since the original action is quadratic, we get the path integral. For convenience, $i\varepsilon$ was not included in the calculations. General formulation of path integral:

$$\int \mathcal{D}\phi^* \mathcal{D}\phi \exp \left[i \int d^4x (\phi^* M \phi + JM) \right] = \mathcal{N} \frac{1}{\det M} \exp(iJM^{-1}J) \quad (5.24)$$

\mathcal{N} is the normalization constant. If we apply the above equation for the scalar Lagrangian, we find:

$$\int \mathcal{D}A \exp(i\Gamma[A]) = \mathcal{N} \int \mathcal{D}A \exp \left[i \int d^4x \left(-\frac{1}{4}F_{\mu\nu}^2 \right) \right] \frac{1}{\det(-D^2 - m^2)} \quad (5.25)$$

In order for this equation to be satisfied, the equation must satisfy that.

$$\exp \left[i\Gamma[A] + i \int d^4x \frac{1}{4} F_{\mu\nu}^2 \right] = \mathcal{N} \frac{1}{\det(-D^2 - m^2)} \quad (5.26)$$

By transforming the determinant, we provide a little more understanding of the equation.

$$i\Gamma[A] + i \int d^4x \frac{1}{4} F_{\mu\nu}^2 - \ln \mathcal{N} = -\ln[\det(-D^2 - m^2)] = -\text{tr}[\ln(-D^2 - m^2)] \quad (5.27)$$

The trace here is a sum of eigenvalues. The trace in our configuration, follows an independent path. Therefore, results are obtained by summing the eigenstates of the positions. After this, using quantum mechanical notation and applying the Schwinger proper time method, the equations can be written as (differentiating with respect to m^2)

$$i\Gamma[A] = \int d^4x \left[-\frac{i}{4} F_{\mu\nu}^2 - \langle x | \ln(-D^2 - m^2) | x \rangle \right] + \ln \mathcal{N} \quad (5.28)$$

$$\begin{aligned} \frac{d}{dm^2} \langle x | \ln(-D^2 - m^2) | x \rangle &= -\langle x | \frac{1}{-D^2 - m^2} | x \rangle \\ &= i \int_0^\infty ds e^{-ism^2} \langle x | e^{-i\hat{H}s} | x \rangle \end{aligned} \quad (5.29)$$

The equation is integrated with respect to m^2 and add the $i\varepsilon$ values, which we ignore for convenience, to the equation, we find the value of $\mathcal{L}_{\text{eff}}(x)$

$$\mathcal{L}_{\text{eff}}^{\text{scl}}(x) = -\frac{1}{4} F_{\mu\nu}^2 - i \int_0^\infty \frac{ds}{s} e^{-s\varepsilon} e^{-ism^2} \langle x | e^{-i\hat{H}s} | x \rangle + \text{const.} \quad (5.30)$$

where the constant can be ignored since it would have no physical effect. Here the Hamiltonian is $\hat{H} = -(\hat{k} - eA(\hat{x}))^2$.

At this point one might interpret the effective Lagrangians obtained in terms of Feynman diagrams. After all this is a perturbative approach and once the term $e^{-i\hat{H}s}$ is

expanded, each term corresponds to a diagram. Let us concentrate on the effective Lagrangian for the fermion case, $\mathcal{L}_{eff}^{frm}(x)$, the one in equation (5.22).

$$\frac{i}{2} \int_0^\infty \frac{ds}{s} e^{-s\varepsilon} e^{-ism^2} \text{Tr}[\langle x | e^{-i\hat{H}s} | x \rangle] = \text{Diagram 1} + \text{Diagram 2} + \text{Diagram 3} + \text{Diagram 4} + \text{Diagram 5} + \dots \quad (5.31)$$

By using the effective Lagrangian in (5.8), a similar interpretation can be done for the complex scalar case as well where the electron loops will be replaced with the scalar loops.

Since we are interested in concentrating on the vacuum energy only, the above expansion should be reduced to the one with no external field interactions (interactions with the photon field A_μ). Hence, for the vacuum energy the relevant quantity for the effective action is $\Gamma[A_\mu = 0] \equiv \Gamma[0]$. In that case the only diagram left *at the leading order* is the first diagram in equation (5.31) for the fermion case. This is indeed the effective Lagrangian term when $e^{-i\hat{H}s} = e^{i\hat{k}^2 s}$ in the limit $A_\mu \rightarrow 0$. This is true for both the scalar and the spinor cases since the Hamiltonians are identical in the limit.

At the end of this section, the vacuum energy of this diagram will be calculated and this will be the bridge to get the effective potential energy density V_{eff} , which is the starting point for the Casimir force calculation once a geometry is chosen. Once this connection is established, in the next section, radiative corrections to the leading order will be considered. Indeed, such diagrams can also be interpreted from the above expansion. For example take the diagram with two external photon legs, the third diagram in equation (5.31). As it is, it indeed defines a fermion loop correction to the photon propagator but if the external lines are connected to each other it turns out to be correction to the vacuum energy, known as the Uehling correction. Similarly, the diagram with four external legs can be treated to be another contribution, known

as the Euler-Heisenberg correction. These two corrections are going to be the subject of the next section.

Let us go back to the vacuum energy calculation from the one-loop consideration as mentioned above. For the complex scalar field case, the calculation will be carried out and the spinor case will be commented since they are almost the same. From the effective Lagrangian $\mathcal{L}_{eff}^{scl}(x)$ from equation (5.30) with $A_\mu \rightarrow 0$, one can write the effective action

$$\begin{aligned}
\Gamma^{scl}[0] &\equiv \int d^4x \mathcal{L}_{eff}^{scl}(x, A_\mu \rightarrow 0) \\
&= -i \int d^4x \int_0^\infty \frac{ds}{s} e^{-s\varepsilon} e^{-ism^2} \langle x | e^{ik^2s} | x \rangle \\
&= -i \int d^4x \int_0^\infty \frac{ds}{s} \int \frac{d^4p}{(2\pi)^4} e^{-s\varepsilon} e^{-ism^2} \langle x | e^{ik^2s} | p \rangle \langle p | x \rangle \\
&= -i \underbrace{\int d^4x}_{=V_4} \int_0^\infty \frac{ds}{s} \int \frac{d^4p}{(2\pi)^4} e^{-s\varepsilon} e^{-ism^2} e^{ip_\mu p^\mu s} \\
&= -iV_4 \int_0^\infty \frac{ds}{s} \int \frac{d^4p}{(2\pi)^4} e^{i(p_\mu p^\mu - m^2 + i\varepsilon)s} \\
&\equiv -V_4 V_{eff}^{scl}
\end{aligned} \tag{5.32}$$

where V_4 is the volume of the 4-dimensional spacetime and V_{eff}^{scl} is the effective potential energy density defined as

$$V_{eff}^{scl} = i \int_0^\infty \frac{ds}{s} \int \frac{d^4p}{(2\pi)^4} e^{i(p_\mu p^\mu - m^2 + i\varepsilon)s} \tag{5.33}$$

At this stage one can directly obtain the effective potential energy density for the fermion case directly from V_{eff}^{scl} . This can be done by simply counting the additional factors that the spinor case has as compared to the scalar one. From equations (5.30) and (5.22), it is evident that

$$\begin{aligned}
V_{eff}^{frm} &= 4 \times \left(-\frac{1}{2}\right) V_{eff}^{scl} \\
&= -2V_{eff}^{scl}
\end{aligned} \tag{5.34}$$

Here the factor 4 is due to the additional Dirac trace and the factor $(-\frac{1}{2})$ due to the difference in the coefficients. The relative minus sign between the scalar and fermion cases originates from the fact that there is a relative minus sign difference between the fermion loop and the scalar loop. The relative factor of two can also be understood. This sign difference would also have some further implications. The nature of the Casimir force originating in each case would be different. If the force turns out to be an attractive one for the scalar case, it would be repulsive for the fermion case.

Now, let us compute the integrals in V_{eff}^{scl} (the $i\varepsilon$ piece will be dropped since it would not play any role for the current discussion);

$$\begin{aligned}
V_{eff}^{scl} &= i \int_0^\infty \frac{ds}{s} \int \frac{d^4 p}{(2\pi)^4} e^{i(p_\mu p^\mu - m^2)s} \\
&= i \int_0^\infty \frac{ds}{s} \int \frac{d^3 \mathbf{p}}{(2\pi)^3} \int \frac{dp_0}{2\pi} \underbrace{e^{i(p_0^2 - \mathbf{p}^2 - m^2)s}}_{p_0 \rightarrow ip_0, dp_0 = idp_0} \\
&= - \int \frac{d^3 \mathbf{p}}{(2\pi)^3} \int_0^\infty \frac{ds}{s} e^{-i(\mathbf{p}^2 + m^2)s} \underbrace{\int \frac{dp_0}{2\pi} e^{ip_0^2 s}}_{= \frac{1}{2\pi} \frac{1}{\sqrt{s}} \Gamma(\frac{1}{2})} \\
&= - \frac{1}{2\pi} \Gamma\left(\frac{1}{2}\right) \int \frac{d^3 \mathbf{p}}{(2\pi)^3} \underbrace{\int_0^\infty \frac{ds}{s^{3/2}} e^{-i(\mathbf{p}^2 + m^2)s}}_{= \sqrt{\mathbf{p}^2 + m^2} \Gamma(-\frac{1}{2})} \\
&= - \frac{1}{2\pi} \underbrace{\Gamma\left(\frac{1}{2}\right) \Gamma\left(-\frac{1}{2}\right)}_{= \sqrt{\pi} (-2\sqrt{\pi})} \int \frac{d^3 \mathbf{p}}{(2\pi)^3} \sqrt{\mathbf{p}^2 + m^2} \\
&= \int \frac{d^3 \mathbf{p}}{(2\pi)^3} \underbrace{\sqrt{\mathbf{p}^2 + m^2}}_{= \omega_p} \tag{5.35}
\end{aligned}$$

which is our final expression² for the effective potential energy density of the vacuum due to a complex scalar field with mass m . Obviously to make an analogy with the photon field, one needs to set $m = 0$. In that case the obtained dispersion relation becomes $\omega_p = |\mathbf{p}|$, which is the expected form for the photon case. As far as the zero-point energy is concerned, a factor of $\frac{1}{2}$ is missing and this is entirely due the fact that the complex scalar field has twice the degrees of freedom that the real one has. Due to this, the scalar analogy for the photon field is always done with the real

² Obviously the calculation has been done by setting the natural units, that is, $\hbar = c = 1$. However, if they are restored, there would be a factor of $\hbar c$ in front of the integral as well as some factors of c inside the square-root.

scalar field instead of a complex one. Of course, later one has to multiply everything by a factor of two to account for the photon's two polarization degrees of freedom.

5.2 Radiative Corrections to the Casimir Force

Even though the Casimir energy itself is indeed a one-loop effect as shown in the previous section, the common practice is to treat it to be as a tree-level process. The electromagnetic field is considered as a superposition of plane waves with frequencies ω_k 's. Then the vacuum energy of the electromagnetic field turns out to be the sum of the zero point energies

$$\frac{1}{2} \int d^3x (\mathbf{E}^2 + \mathbf{B}^2) = \sum_{\lambda=1,2} \sum_k \frac{\omega_{k\lambda}}{2} \quad (5.36)$$

where λ represents the polarization of the photon. Then one can proceed as outlined in Chapters 3 and 4. There are some interests in dealing with the radiative corrections to the Casimir force. This remains mostly theoretical pursuit since the corrections are rather minuscule numerically so that it would be difficult to see any significant deviations.

One way to calculate the radiative corrections is to concentrate on the effective QED by assuming energies, relevant to the process at hand, much smaller than the mass of electron m . Under such circumstances, one would make an expansion in the inverse powers of m . There are indeed two relevant corrections up to $\mathcal{O}(\alpha_{em}^2)$ [32]:

$$\begin{aligned} \mathcal{L}_{\text{eff}} &= \mathcal{L}_0(A_\mu) + \mathcal{L}_{Ueh} + \mathcal{L}_{EH} \\ \mathcal{L}_{Ueh} &= \frac{\alpha_{em}}{60\pi m^2} F_{\mu\nu} \partial_\beta \partial^\beta F^{\mu\nu} \\ \mathcal{L}_{EH} &= \frac{\alpha_{em}^2}{90m^4} \left[(F_{\mu\nu} F^{\mu\nu})^2 + \frac{7}{4} (F_{\mu\nu} \tilde{F}^{\mu\nu})^2 \right] \end{aligned} \quad (5.37)$$

where \mathcal{L}_{Ueh} is known as the Uehling Lagrangian which is the lowest order correction and \mathcal{L}_{EH} is the well known Euler-Heisenberg term³. $\tilde{F}_{\mu\nu} = \frac{1}{2} \epsilon_{\mu\nu\alpha\beta} F^{\alpha\beta}$ is the dual

³ In this form of the Lagrangian the electromagnetic field A_μ is assumed not to be dynamical

field strength tensor.

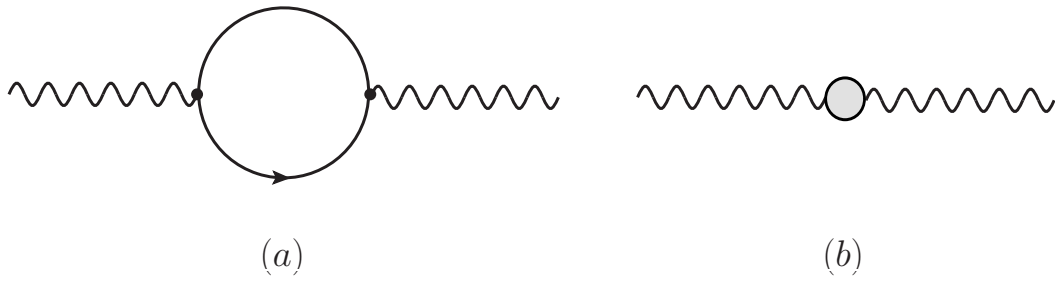


Figure 5.1: In the panel (a), the one-loop Feynman diagram responsible for the Uehling term before the electron field is integrated out is shown. In the panel (b), the electron loop is shrunk to a point.

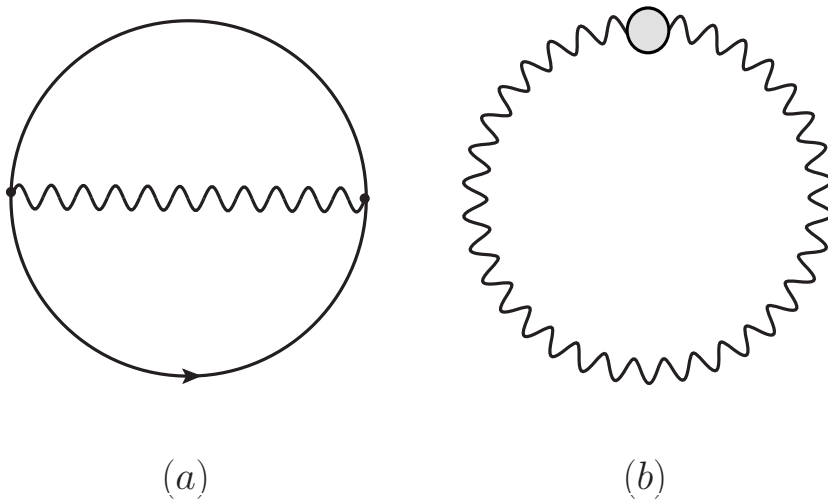


Figure 5.2: In the panel (a), the Uehling diagram contributing the vacuum energy at the $\mathcal{O}(\alpha_{em})$ order is shown, obtained from from the panel (a) of Fig. 5.1 by connecting the external photon lines with each other. In the panel (b), the same but this time by using the the panel (b) of Fig. 5.1.

As far as the Uehling correction [33] is concerned it is nothing but the one-loop electron correction to the photon propagator as shown in the left panel of Fig. 5.1 since the term is proportional to the photon field quadratically and once the loop shrinks to a point in the limit $k^2 \ll m^2$ it produces \mathcal{L}_{Ueh} term at the lowest order within the effective QED, which indeed corresponds to the diagram in the panel (b) of Fig. 5.1

The Uehling diagram contributing the vacuum energy at the $\mathcal{O}(\alpha_{em})$ order can be

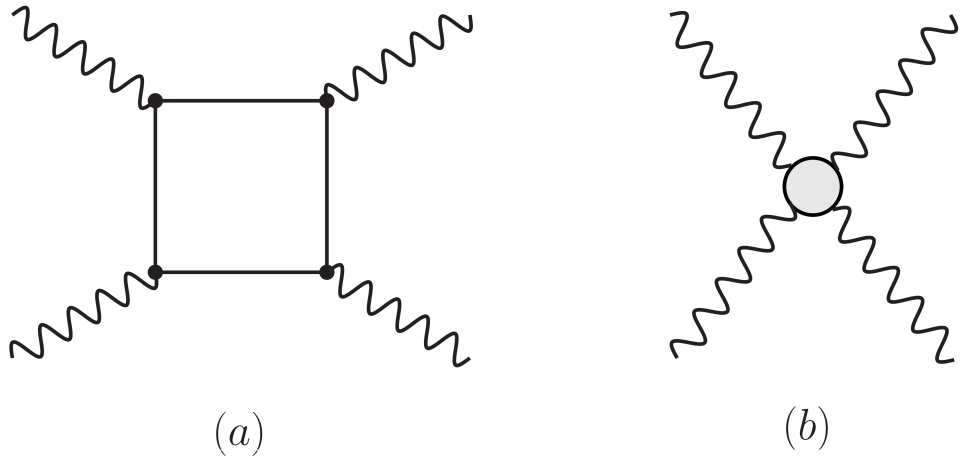


Figure 5.3: In the panel (a), the one-loop Feynman diagram responsible for the Euler-Heisenberg term before the electron field is integrated out is shown. In the panel (b), the electron box is shrunk to a point.

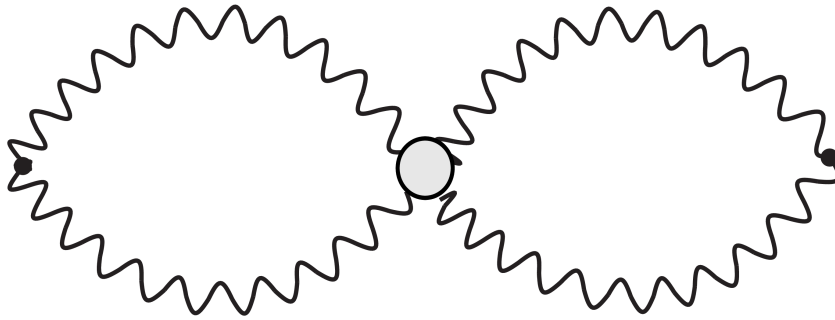


Figure 5.4: This is the Euler-Heisenberg diagram contributing the vacuum energy at the $\mathcal{O}(\alpha_{em}^2)$ order. Indeed this is obtained from the panel (b) of Fig. 5.3 by connecting the external photon lines with each other.

obtained from the panel (a) of Fig. 5.1 by connecting the external photon lines with each other. In the panel (b), the same contribution but this time by using the diagram in the panel (b) of Fig. 5.1. These two diagrams are depicted in the panels (a) and (b) of Fig. 5.2, respectively. The Uehling correction is not going to be pursued further here since such a Lagrangian term can be effectively eliminated by imposing the wave equation for the electromagnetic field without any source, namely $\partial_\alpha \partial^\alpha F^{\mu\nu} = 0$.

In the case of the Euler-Heisenberg correction [34, 35], it involves four photon fields with an effective self interaction as depicted in the panel (b) of Fig. 5.3. The full diagram is also shown in the panel (a) of Fig. 5.3. As compared to the Uehling term, the Euler-Heisenberg interaction could also give contribution to the photon propagator, which is a photon tadpole diagram with an effective four-point vertex factor. Like in the case of Uehling, there is a correction to the vacuum energy from the Euler-Heisenberg term and the corresponding diagram in the effective theory is shown in Fig. 5.4.

To compute the Euler-Heisenberg correction, it would be useful to express the Euler-Heisenberg Lagrangian in terms of the electric and magnetic fields (\mathbf{E} , \mathbf{B})

$$\begin{aligned}\mathcal{L}_{EH} &= \frac{\alpha_{em}^2}{90m^4} \left[(F_{\mu\nu} F^{\mu\nu})^2 + \frac{7}{4} (F_{\mu\nu} \tilde{F}^{\mu\nu})^2 \right] \\ &= \frac{2\alpha_{em}^2}{45m^4} \left[(\mathbf{E}^2 - \mathbf{B}^2)^2 + 7(\mathbf{E} \cdot \mathbf{B})^2 \right]\end{aligned}\quad (5.38)$$

Recall that

$$\begin{aligned}F_{\mu\nu} F^{\mu\nu} &= 2(\mathbf{E}^2 - \mathbf{B}^2) \\ F_{\mu\nu} \tilde{F}^{\mu\nu} &= -4 \mathbf{E} \cdot \mathbf{B}\end{aligned}\quad (5.39)$$

The energy density correction $\Delta\mathcal{E}$ due to the Euler-Heisenberg interaction becomes $\Delta\mathcal{E} = -\mathcal{L}_{EH}$ so that the contribution to the Casimir energy from the Euler-Heisenberg Lagrangian is [32]

$$\begin{aligned}
\Delta E_{\text{EH}} &= \int d^3 \mathbf{x} \langle \Delta \mathcal{E} \rangle \\
&= -\frac{2\alpha_{em}^2}{45m^4} \int d^3 \mathbf{x} \langle (\mathbf{E}^2 - \mathbf{B}^2)^2 + 7(\mathbf{E} \cdot \mathbf{B})^2 \rangle
\end{aligned} \tag{5.40}$$

To compute this correction explicitly, the following electric and magnetic field fluctuations need to be computed: $\langle \mathbf{E}^4 \rangle$, $\langle \mathbf{E}^2 \rangle$, $\langle \mathbf{B}^4 \rangle$, $\langle \mathbf{B}^2 \rangle$, $\langle \mathbf{E}^2 \mathbf{B}^2 \rangle$, and $\langle (\mathbf{E} \cdot \mathbf{B})^2 \rangle$. For example, let us express $\langle E_x(x)E_x(x') \rangle$ by using the photon propagator from x to x' together with the boundary conditions at $z = 0$ and $z = a$.

$$\begin{aligned}
\langle E_x(x)E_x(x') \rangle &= \frac{2}{a} \int \frac{d\omega}{2\pi} e^{-i\omega(t-t')} \int \frac{d^2 \mathbf{k}_\perp}{(2\pi)^2} \frac{i}{\mathbf{k}_\perp^2} e^{-i\mathbf{k}_\perp \cdot (\mathbf{x}_\perp - \mathbf{x}'_\perp)} \\
&\quad \times \sum_{n=1} \frac{w^2 k_y^2 + k_x^2 k_n^2}{\omega^2 - k_\perp^2 - k_n^2} \sin(k_n z) \sin(k_n z')
\end{aligned} \tag{5.41}$$

When the point $x' \rightarrow x$, one gets after carrying the ω integral

$$\langle E_x^2 \rangle = \frac{1}{a} \int \frac{d^2 \mathbf{k}_\perp}{(2\pi)^2} \sum_{n=1} \frac{k_y^2 + k_n^2}{w_n} \sin^2(k_n z) \tag{5.42}$$

where $\omega_n \equiv \sqrt{\mathbf{k}_\perp^2 + k_n^2}$. A similar calculation for $\langle E_y^2 \rangle$ can be done with the final result

$$\langle E_y^2 \rangle = \frac{1}{a} \int \frac{d^2 \mathbf{k}_\perp}{(2\pi)^2} \sum_{n=1} \frac{k_x^2 + k_n^2}{w_n} \sin^2(k_n z) \tag{5.43}$$

so that one gets

$$\begin{aligned}
\langle \mathbf{E}_\perp^2 \rangle &= \frac{1}{a} \int \frac{d^2 \mathbf{k}_\perp}{(2\pi)^2} \sum_{n=1} \frac{\mathbf{k}_\perp^2 + 2k_n^2}{w_n} \sin^2(k_n z) \\
&= \frac{1}{a} \int \frac{d^2 \mathbf{k}_\perp}{(2\pi)^2} \sum_{n=1} \left(w_n + \frac{k_n^2}{w_n} \right) \sin^2(k_n z)
\end{aligned} \tag{5.44}$$

In a similar fashion, for example one could write for $\langle E_n(x)E_n(x') \rangle$ as

$$\begin{aligned} \langle E_n(x)E_n(x') \rangle &= \frac{2}{a} \int \frac{d\omega}{2\pi} e^{-i\omega(t-t')} \int \frac{d^2\mathbf{k}_\perp}{(2\pi)^2} e^{-i\mathbf{k}_\perp \cdot (\mathbf{x}_\perp - \mathbf{x}'_\perp)} \\ &\times \sum_{n=1} \frac{i\mathbf{k}_\perp^2}{\omega^2 - k_\perp^2 - k_n^2} \cos(k_n z) \cos(k_n z') \end{aligned} \quad (5.45)$$

Then

$$\langle \mathbf{E}_n^2 \rangle = \frac{1}{a} \int \frac{d^2\mathbf{k}_\perp}{(2\pi)^2} \sum_{n=1} \left(w_n - \frac{k_n^2}{w_n} \right) \cos^2(k_n z) \quad (5.46)$$

One can further show that

$$\langle \mathbf{B}_x^2 \rangle = \langle \mathbf{B}_y^2 \rangle = -\langle \mathbf{E}_n^2 \rangle \quad \langle \mathbf{B}_n^2 \rangle = -\langle \mathbf{E}_x^2 \rangle \quad (5.47)$$

To carry out \mathbf{k}_\perp integrals, one may use the following

$$\int \frac{d^2k_T}{(2\pi)^2} \frac{1}{\omega_n^m} = \frac{k_n^{2-m}}{4\pi} \frac{\Gamma\left(\frac{m-2}{2}\right)}{\Gamma\left(\frac{m}{2}\right)} \equiv C_m \quad (5.48)$$

Using the formula, we may write

$$\langle \mathbf{E}_\perp^2 \rangle = \frac{1}{a} \sum_{n=1} \left(C_{-1} + k_n^2 C_1 \right) \sin^2(k_n z) \quad (5.49)$$

Here one may compute

$$\begin{aligned} C_{-1} &= \frac{k_n^3 \Gamma(-3/2)}{4\pi \Gamma(-1/2)} = -\frac{k_n^3}{6\pi} \\ C_1 &= \frac{k_n \Gamma(-1/2)}{4\pi \Gamma(1/2)} = -\frac{3k_n}{6\pi} \end{aligned} \quad (5.50)$$

Thus one gets

$$\begin{aligned}
\langle \mathbf{E}_\perp^2 \rangle &= -\frac{2}{3\pi a} \sum_{n=1} k_n^3 \sin^2(k_n z) \\
&= -\frac{2\pi^2}{3a^4} \sum_{n=1} n^3 \sin^2(n\pi z/a)
\end{aligned} \tag{5.51}$$

Similarly

$$\langle \mathbf{E}_n^2 \rangle = \frac{\pi^2}{3a^4} \sum_{n=1} n^3 \cos^2(n\pi z/a) \tag{5.52}$$

Since to get ΔE_{EH} the volume integral needs to be computed. For example

$$\begin{aligned}
\int d^3 \mathbf{x} \langle \mathbf{E}_\perp^2 \rangle &= -A \frac{\pi^2}{3a^4} \sum_{n=1} n^3 \underbrace{\int_0^a dz \sin^2(n\pi z/a)}_{a/2} \\
&= -A \frac{\pi^2}{6a^3} \underbrace{\sum_{n=1} n^3}_{\zeta(-3)=1/120} \\
&= -\frac{A\pi^2}{720 a^3}
\end{aligned} \tag{5.53}$$

where $\int dx dy \equiv A$. In a similar fashion

$$\int d^3 \mathbf{x} \langle \mathbf{E}_n^2 \rangle = \frac{A\pi^2}{1440 a^3} \tag{5.54}$$

To be able to get a final formula for ΔE_{EH} , one still needs combinations like $\langle E_i^2 E_j^2 \rangle$ which can be expressed as

$$\langle V_j^2 V_k^2 \rangle = \langle V_j^2 \rangle \langle V_k^2 \rangle + 2\delta_{jk} \langle V_j^2 \rangle^2, \quad V = E, B \tag{5.55}$$

Computing all the other combinations and plugging them into equation (5.40), the final formula becomes

$$\Delta E_{\text{EH}} = -\frac{11\alpha_{em}^2 \pi^4}{3888000} \frac{1}{m^4 a^7} \tag{5.56}$$

CHAPTER 6

CONCLUSION

In this thesis, we investigated the relation between Van der Waals forces and Casimir forces. In specific, we have looked closely at some approaches to understand the relationship between them. We analyzed London's and Casimir's views on the distance dependence of these forces and investigated the retardation term Polder introduced to address relativistic correction in the theory. We gave a brief overview about the definition of the Casimir force and its emergence by examining the relationship of this force with magnetic or electric fields.

After a brief look at the history, we examined the harmony of the theory with various experiments. We shared the results of the experiments in different geometries. We analyzed Sparnaay's experimental data by fitting the theoretical expression of the Casimir force to his results.

In Chapter 3, we looked at the calculation of the Casimir force for the case of two parallel plates. Starting from the fact that the vacuum energy is related to Planck's half quanta, we determined the energy levels for the vacuum between the plates and consequently derived an expression for the Casimir force. We have shown that the energy cannot reach a finite value when we assume all the dimensions are, so we showed that it is necessary to apply a cut off range. In addition to this, we have reached the desired result by showing the concept of polarization states and energy-force relationship.

Since it was necessary to make some modifications in the basic theory in order to arrive at a finite energy value, the next chapter was to calculate Casimir force using two important regularization methods. In the dimensional regularization method, a

transverse dimension D is defined as a continuous complex variable and its possible values are subsequently constrained using properties of Γ function. By doing so, we arrive at the same result from Chapter 3. For the Zeta regularization method, we first define the Riemann Zeta function $\zeta(s)$. Then, in order to avoid divergent results, we made use of Zeta regulator after which we arrived at the result that we expected.

In Chapter 5, by defining the concept of effective action, we examined its relationship with full action theory. We observed the effects of Schwinger proper time and path integral concepts on effective action. We computed Lagrangian for scalar and spinor case using Schwinger's formulation. After these calculations, we calculated the effective potential density in order to reach the Casimir force and calculated what would happen in the absence of mass(photon case). In addition to these, we did radiative correction for Casimir force in this chapter. We have defined the terms Uehling Lagrangian and Euler-Heisenberg Lagrangian using Feynman diagrams and theoretical interests.

Last but not least, while the energy density correction give us some idea about the one loop level, we also need to study dark photon phenomena. Indeed the effect of the so-called dark sector in the form of a $U(1)$ gauge theory on the casimir force between two parallel plates. As such, the study of dark sector will be the next stage of the author's research.

REFERENCES

- [1] K. Milton and P. Milonni, “The casimir effect: Physical manifestations of zero-point energy,” *Physics Today*, vol. 56, pp. 49–50, 01 2003.
- [2] G. Klimchitskaya and V. Mostepanenko, “Casimir and van der waals forces: Advances and problems,” *Proceedings of Peter the Great St. Petersburg Polytechnic University*, p. 41–65, Jun 2015.
- [3] S. K. Lamoreaux, “Demonstration of the casimir force in the 0.6 to $6\mu\text{m}$ range,” *Phys. Rev. Lett.*, vol. 78, pp. 5–8, Jan 1997.
- [4] U. Mohideen and A. Roy, “Precision measurement of the casimir force from 0.1 to $0.9\mu\text{m}$,” *Phys. Rev. Lett.*, vol. 81, pp. 4549–4552, Nov 1998.
- [5] M. Sparnaay, “Measurements of attractive forces between flat plates,” *Physica*, vol. 24, no. 6, pp. 751 – 764, 1958.
- [6] R. S. Decca, D. López, E. Fischbach, and D. E. Krause, “Measurement of the casimir force between dissimilar metals,” *Phys. Rev. Lett.*, vol. 91, p. 050402, Jul 2003.
- [7] D. Iannuzzi, M. Lisanti, and F. Capasso, “Effect of hydrogen-switchable mirrors on the casimir force,” *Proceedings of the National Academy of Sciences of the United States of America*, vol. 101, pp. 4019–23, 04 2004.
- [8] P. H. G. M. van Blokland and J. T. G. Overbeek, “van der waals forces between objects covered with a chromium layer,” *J. Chem. Soc., Faraday Trans. I*, vol. 74, pp. 2637–2651, 1978.
- [9] T. Ederth, “Template-stripped gold surfaces with 0.4-nm rms roughness suitable for force measurements: Application to the casimir force in the 20–100-nm range,” *Phys. Rev. A*, vol. 62, p. 062104, Nov 2000.

- [10] F. Chen, U. Mohideen, G. L. Klimchitskaya, and V. M. Mostepanenko, “Demonstration of the lateral casimir force,” *Phys. Rev. Lett.*, vol. 88, p. 101801, Feb 2002.
- [11] G. Bressi, G. Carugno, R. Onofrio, and G. Ruoso, “Measurement of the casimir force between parallel metallic surfaces,” *Phys. Rev. Lett.*, vol. 88, p. 041804, Jan 2002.
- [12] R. Decca, D. López, E. Fischbach, G. Klimchitskaya, D. Krause, and V. Mostepanenko, “Precise comparison of theory and new experiment for the casimir force leads to stronger constraints on thermal quantum effects and long-range interactions,” *Annals of Physics*, vol. 318, Jul 2005.
- [13] F. Chen, U. Mohideen, G. L. Klimchitskaya, and V. M. Mostepanenko, “Experimental test for the conductivity properties from the casimir force between metal and semiconductor,” *Phys. Rev. A*, vol. 74, p. 022103, Aug 2006.
- [14] H. B. Chan, Y. Bao, J. Zou, R. A. Cirelli, F. Klemens, W. M. Mansfield, and C. S. Pai, “Measurement of the casimir force between a gold sphere and a silicon surface with nanoscale trench arrays,” *Physical Review Letters*, vol. 101, Jul 2008.
- [15] G. L. Klimchitskaya, U. Mohideen, and V. M. Mostepanenko, “The casimir force between real materials: Experiment and theory,” *Rev. Mod. Phys.*, vol. 81, pp. 1827–1885, Dec 2009.
- [16] A. Canaguier-Durand, P. A. M. Neto, A. Lambrecht, and S. Reynaud, “Thermal casimir effect in the plane-sphere geometry,” *Physical Review Letters*, vol. 104, Jan 2010.
- [17] P. J. van Zwol, V. B. Svetovoy, and G. Palasantzas, “Characterization of optical properties and surface roughness profiles: The casimir force between real materials,” *Lecture Notes in Physics*, p. 311–343, 2011.
- [18] R. O. Behunin, F. Intravaia, D. A. R. Dalvit, P. A. M. Neto, and S. Reynaud, “Modeling electrostatic patch effects in casimir force measurements,” *Phys. Rev. A*, vol. 85, p. 012504, Jan 2012.

- [19] G. L. KLIMCHITSKAYA, M. BORDAG, and V. M. MOSTEPANENKO, “Comparison between experiment and theory for the thermal casimir force,” *International Journal of Modern Physics A*, vol. 27, p. 1260012, Jun 2012.
- [20] G. Bimonte, D. López, and R. S. Decca, “Isoelectronic determination of the thermal casimir force,” *Physical Review B*, vol. 93, May 2016.
- [21] G. Bimonte, “Going beyond PFA: A precise formula for the sphere-plate Casimir force,” *EPL*, vol. 118, no. 2, p. 20002, 2017.
- [22] A. Le Cunuder, A. Petrosyan, G. Palasantzas, V. Svetovoy, and S. Ciliberto, “Measurement of the casimir force in a gas and in a liquid,” *Phys. Rev. B*, vol. 98, p. 201408, Nov 2018.
- [23] G. Bimonte, “Casimir effect between superconductors,” *Physical Review A*, vol. 99, May 2019.
- [24] A. Lambrecht, “The casimir effect: A force from nothing,” *Physics World*, vol. 15, 09 2002.
- [25] “Plancks half-quanta: A history of the concept of zero-point energy,” *The Golden Age of Theoretical Physics*, p. 56–93, 2001.
- [26] G. Leibbrandt, “Introduction to the technique of dimensional regularization,” *Rev. Mod. Phys.*, v. 47, no. 4, pp. 849-876, 10 1975.
- [27] E. ELIZALDE, “Zeta function regularization in casimir effect calculations and j. s. dowker’s contribution,” *International Journal of Modern Physics A*, vol. 27, p. 1260005, Jun 2012.
- [28] D. Ray and I. Singer, “R-torsion and the laplacian on riemannian manifolds,” *Advances in Mathematics*, vol. 7, no. 2, pp. 145 – 210, 1971.
- [29] T. Peters, “Quantum field theory and the standard model, by matthew d. schwartz,” *Contemporary Physics*, vol. 56, no. 1, pp. 101–102, 2015.
- [30] D. J. Toms, *The Schwinger Action Principle and Effective Action*. Cambridge Monographs on Mathematical Physics, Cambridge University Press, 2007.
- [31] M. D. Schwartz, “Quantum Field Theory and the Standard Model,” 2013.

- [32] X. Kong and F. Ravndal, “Quantum corrections to the qed vacuum energy,” *Nuclear Physics B*, vol. 526, no. 1, pp. 627–656, 1998.
- [33] E. A. Uehling, “Polarization effects in the positron theory,” *Phys. Rev.*, vol. 48, pp. 55–63, 1935.
- [34] H. Euler, “On the scattering of light by light according to Dirac’s theory,” *Annalen Phys.*, vol. 26, no. 5, pp. 398–448, 1936.
- [35] W. Heisenberg and H. Euler, “Consequences of Dirac’s theory of positrons,” *Z. Phys.*, vol. 98, no. 11-12, pp. 714–732, 1936.

APPENDIX A

DERIVATION OF \mathcal{D}^2

The Dirac equation for the spinor ψ with an electromagnetic interaction through minimal substitution can be written as

$$(i\gamma^\mu D_\mu - m)\psi = 0 \quad (\text{A.1})$$

where

$$D_\mu \psi = (\partial_\mu - ie Q_f A_\mu)\psi$$

Here Q_f is the electric charge of the fermion field in units of e . Define $C_\mu \equiv iD_\mu$ and multiply equation (A.1) from left by $\mathcal{C} + m$ one gets

$$\begin{aligned} (\mathcal{C} + m)(\mathcal{C} - m)\psi &= 0 \\ (\mathcal{C}^2 - m^2)\psi &= 0 \end{aligned} \quad (\text{A.2})$$

Let us expand \mathcal{C}^2 term:

$$\begin{aligned} \mathcal{C}^2 &= C_\mu C_\nu \gamma^\mu \gamma^\nu \\ &= \frac{1}{2} \left(\{C_\mu, C_\nu\} + [C_\mu, C_\nu] \right) \frac{1}{2} \left(\{\gamma^\mu, \gamma^\nu\} + [\gamma^\mu, \gamma^\nu] \right) \\ &= \frac{1}{4} \left(\{C_\mu, C_\nu\} \{\gamma^\mu, \gamma^\nu\} + [C_\mu, C_\nu] [\gamma^\mu, \gamma^\nu] \right) \\ &= \frac{1}{2} \{C_\mu, C_\nu\} g^{\mu\nu} - \frac{i}{2} [C_\mu, C_\nu] \sigma^{\mu\nu} \end{aligned} \quad (\text{A.3})$$

where there is no cross terms due to symmetric \times antisymmetric combination. Moreover the following identities $\{\gamma^\mu, \gamma^\nu\} = 2g^{\mu\nu}$ and $[\gamma^\mu, \gamma^\nu] = -2i\sigma^{\mu\nu}$ are employed.

The term $\{C_\mu, C_\nu\}g^{\mu\nu} = -2D_\mu^2$. The second term becomes

$$\begin{aligned}
[C_\mu, C_\nu] &= [iD_\mu, iD_\nu] \\
&= [i\partial_\mu + eQ_f A_\mu, i\partial_\nu + eQ_f A_\nu] \\
&= [i\partial_\mu, f_\nu] - [i\partial_\nu, f_\mu] \\
&= i(\partial_\mu f_\nu - \partial_\nu f_\mu) \\
&= if_{\mu\nu}
\end{aligned} \tag{A.4}$$

Here $f_{\mu\nu} = \partial_\mu f_\nu - \partial_\nu f_\mu$ and $f_\mu \equiv eQ_f A_\mu$. Hence

$$[C_\mu, C_\nu] = ieQ_f F_{\mu\nu} \tag{A.5}$$

where $F_{\mu\nu}$ is the field strength tensor. Combining terms in equation (A.3) yields

$$\mathcal{Q}^2 \equiv -\mathcal{D}^2 = -D_\mu^2 + \frac{e}{2}Q_f F_{\mu\nu}\sigma^{\mu\nu} \tag{A.6}$$

which is the desired result.